Layering transitions at an interface

1986 J. Phys. A: Math. Gen. 19 3165

(http://iopscience.iop.org/0305-4470/19/15/037)

J. Phys. A: Math. Gen. 19 (1986) 3165-3184. Printed in Great Britain

Layering transitions at an interface

K Armitstead, J M Yeomans and P M Duxbury

Department of Theoretical Physics, University of Oxford, 1 Keble Road, Oxford OX1 3NP, UK

Received 1 January 1986

Abstract. Low temperature series are used to analyse the wetting of an interface in the three-dimensional three-state chiral clock model. When the calculation is taken to general order using a matrix formulation, a large number of layering transitions are found as a function of the chiral field.

1. Introduction

Surface and interface properties are the subject of considerable interest at present. Research into wetting, surface reconstruction and interfacial adsorption is of relevance in many physical and biological fields (de Gennes 1985, Lipowsky 1985, Telo da Gama 1985). In this paper our aim is to study interfacial wetting in a three-dimensional spin model, the chiral clock model (Huse 1981, Ostlund 1981). We show, using series methods at low temperatures, that the interface wets through a large number of first-order phase transitions.

The three-state chiral clock model is defined by the Hamiltonian

$$H = -J_0 \sum_{\langle ij \rangle}^{\perp} \cos[2\pi(n_i - n_j)/3] - J \sum_{\langle ij \rangle}^{\parallel} \cos[2\pi(n_i - n_j + \Delta)/3] \tag{1}$$

where $n_i = 0, 1, 2$ is a variable on each site, i, of a cubic lattice. The first sum is taken over nearest neighbours within two-dimensional layers, whereas the second is between nearest neighbours along the perpendicular axial direction. The ground state therefore has ferromagnetic layers, although the value of n_i may vary from layer to layer: for $\Delta < \frac{1}{2}$ the ordering between layers is ferromagnetic; for $\Delta > \frac{1}{2}$, however, there is a chiral ground state, ...012 012 012...

To study the interface properties of the three-state chiral clock model (Huse and Fisher 1984), we introduce an interface perpendicular to the chiral direction by setting the spins at $\pm\infty$ to the values 0 and 2 respectively. This introduces a 0:2 interface for sufficiently small Δ. As Δ is increased, however, the energy of a 0:1 interface (and equivalently 1:2 and 2:0) decreases, whereas that of a 0:2 interface increases. Hence it becomes favourable at a certain value, $\Delta = \frac{1}{4}$, for the interface to wet and for the simple 0:2 interface to be replaced by the configuration 0:11...11:2. Note that this is a purely energetic (zero temperature) argument and that the number of ones between the boundaries is arbitrary.

At finite temperature entropy contributions will also be important. It is the aim of this paper to show that these determine n, the number of layers with $n_i = 1$, in the region of $\Delta = \frac{1}{4}$ where the interface wets. We shall show, using a low temperature series

0305-4470/86/153165+20$02.50

expansion (Fisher and Selke 1980, 1981), that the wetting takes place through a series of first-order transitions with n increasing in integer steps and shall find the width in Δ of each interfacial phase.

The next section of this paper is devoted to describing the low temperature expansion and giving explicit results to third order. Hence we show how the series of interface transitions is built up. To this order we can see $n=1$ and $n=2$ appearing. To go further, however, and construct the complete series of phases it is necessary to pick out and compute the relevant terms in the low temperature expansion to all orders. The results of the general order calculation are presented in § 3 with the details of the matrix technique used being postponed to the appendices. Section 4 provides a conclusion where a comparison to similar wetting phenomena is given.

2. Low temperature expansion

To determine the behaviour of the interface in the vicinity of $\Delta=\frac{1}{4}$ we use a low temperature series technique and expand about all possible ground states. The standard low temperature expansion (Domb 1960) follows from a decomposition of the partition function

$$Z_N(n)=\exp[-NE_0(n)/k_BT]\left(1+\sum_{m=1}^{\infty}\Delta Z_N^{(m)}\right) \tag{2}$$

where $\Delta Z_N^{(m)}$ is the total contribution from states with m overturned spins, E_0 is the ground state energy per spin and N is the number of spins in the lattice. Using the linked cluster theorem (Domb 1960) the reduced free energy per spin is then given by

$$F=-\frac{F_N(n)}{Nk_BT}=-\frac{E_0}{k_BT}+\frac{\Sigma'\,\Delta Z_N^{(m)}}{N} \tag{3}$$

where $\Sigma'\,\Delta Z_N^{(m)}$ now only contains terms linear in N.

We first establish a notation for the primitive Boltzmann factors corresponding to single spin flips which appear in (3). It is useful to define

$$\begin{aligned} &K_0=J_0/k_BT \qquad K=J/k_BT \\ &\delta=\Delta-\tfrac{1}{4} \qquad c=\cos(2\pi\delta/3) \qquad s=\sin(2\pi\delta/3) \end{aligned} \tag{4}$$

where k_B is Boltzmann's constant and T is the temperature. Then changing an in-layer bond from ferromagnetic to antiferromagnetic corresponds to a factor

$$\omega=\exp(-3K_0/2). \tag{5}$$

Two independent Boltzmann weights are needed to describe the effects of flipping spins on axial bonds:

$$\begin{aligned} &0\text{-}0\rightarrow 0\text{-}1: \qquad x=\exp[\tfrac{1}{2}K(3s-\sqrt{3}c)] \\ &0\text{-}0\rightarrow 0\text{-}2: \qquad y=\exp[-\sqrt{3}cK] \\ &0\text{-}1\rightarrow 0\text{-}2: \qquad x^{-1}y=\exp[\tfrac{1}{2}K(-\sqrt{3}c-3s)]. \end{aligned} \tag{6}$$

(All other possibilities follow immediately from these equations when the symmetries of the different spin states are considered.)

As we aim to establish the equilibrium position of the interfaces imposed on the system, it is most convenient to calculate F_n-F_∞, where F_n is the reduced free energy of the system when n layers of ones appear at the interface; this is because most graphs

cancel out when considering this free energy difference and the resulting counts depend only on the number of spins in the interface. We describe in some detail the results of the low temperature expansion up to third order to clarify the method of calculation and the notation used.

2.1. Ground state

From (1) it follows immediately that

$$(E_n - E_\infty)/k_B T = 3sK \qquad n = 0 \tag{7a}$$

$$= 0 \qquad n \geq 1 \tag{7b}$$

showing that the interface wets at $\Delta = \frac{1}{4}$, and that, for $\Delta > \frac{1}{4}$, all values of $n \neq 0$ correspond to the same interface energy.

2.2. First order

The first-order contributions to $F_0 - F_\infty$ and $F_1 - F_\infty$ are shown in tables 1(*a*) and (*b*) respectively. The first column in the table shows the spin to be flipped; spins in different environments must be considered separately as they correspond to different Boltzmann weights. The second column gives the count per interface spin corresponding to each configuration. Only the term proportional to M, the number of spins per layer, is quoted as those terms proportional to higher-order powers of M and to N drop out when the linked cluster theorem is used in the expansion of the free energy. The weights are given in the third column of the table. $q_\perp$ is the number of nearest neighbours within a layer; for our case of the simple cubic lattice, $q_\perp = 4$. A moment's thought shows that to this order $F_n - F_\infty = 0$, $n \geq 2$, because no single flip can span the distance between the interfaces and hence distinguish between the different values of n.

Summing the contributions in the table gives

$$F_0^{(1)} - F_\infty^{(1)} = (-2 + 2x^2y^{-1} + 4xy - 4x^{-1}y^2)\omega^{q_\perp} \tag{8a}$$

$$F_1^{(1)} - F_\infty^{(1)} = (-2 + 2x^{-2}y + 2xy - 2x^{-1}y^2)\omega^{q_\perp} \tag{8b}$$

$$F_n^{(1)} - F_\infty^{(1)} = 0 \qquad n \geq 2. \tag{8c}$$

Table 1.

(*a*) First-order contributions to $F_0 - F_\infty$.

Configuration	Count	Boltzmann weight
002	2	$(1 + x^2y^{-1})\omega^{q_\perp}$
001	−4	$(1 + x^{-1}y^2)\omega^{q_\perp}$
000	2	$2xy\omega^{q_\perp}$

(*b*) First-order contribution to $F_1 - F_\infty$.

Configuration	Count	Boltzmann weight
001	−2	$(1 + x^{-1}y^2)\omega^{q_\perp}$
012	1	$(2x^{-2}y)\omega^{q_\perp}$
000	1	$2xy\omega^{q_\perp}$

We may write

$$y = x^{2+\alpha} \tag{9}$$

and, noting from (6) that

$$\alpha \log x = -3Ks \tag{10}$$

expand (7) and (8) to leading order to give

$$F_0 - F_\infty = -3Ks + O(\omega^{2q_- - 1}) \tag{11a}$$

$$F_1 - F_\infty \sim O(\omega^{2q_\perp - 1}) \tag{11b}$$

assuming, as will be shown to be consistent later, $\alpha \log x \sim O(\omega^{q_\perp - 1})$. Therefore, to this order, the free energy of the interface is independent of the value of n at $\Delta = \frac{1}{4}$.

2.3. Second order

The second-order contributions to the free energy differences $F_0 - F_\infty$, $F_1 - F_\infty$ and $F_2 - F_\infty$ are shown in tables 2(*a*), (*b*) and (*c*). Boltzmann weights now depend on the relative positions of the two flipped spins. To emphasise the pattern in successive terms of the expansion we have divided the contributing graphs into connected graphs grouped with their decompositions. Summing contributions in the tables gives

$$\begin{aligned} F_0^{(2)} - F_\infty^{(2)} = {} & (-4 + 4x^4y^{-2} + 8x^2y^2 - 8x^{-2}y^4)\omega^{2q_\perp - 2} + (-16x^{-1}y^2 + 8x^2y^{-1} + 8x^2y^2)\omega^{2q_\perp - 1} \\ & + (4 - 7x^2y^{-1} - 6x^4y^{-2} + 5xy + 14x^{-1}y^2 - x^3 - 32x^2y^2 + 11y^3 \\ & + 12x^{-2}y^4)\omega^{2q_-} \end{aligned} \tag{12a}$$

$$\begin{aligned} F_1^{(2)} - F_\infty^{(2)} = {} & (-4 + 4x^{-4}y^2 - 4x^{-2}y^4 + 4x^2y^2)\omega^{2q_\perp - 2} + (4x^{-4}y^2 - 8x^{-1}y^2 + 4x^2y^2)\omega^{2q_\perp - 1} \\ & + (7 - 2x^{-2}y - 10x^{-4}y^2 + 12x^{-1}y^2 + 2x^3 - 4x^{-3}y^3 + 6y^3 + 7x^{-2}y^4 \\ & - 18x^2y^2)\omega^{2q_-} \end{aligned} \tag{12b}$$

$$F_2^{(2)} - F_\infty^{(2)} = (-3 + 3x^{-2}y + 4xy - 5x^{-1}y^2 + x^3 + 5y^3 - x^{-2}y^4 - 4x^2y^2)\omega^{2q_-} \tag{12c}$$

$$F_n^{(2)} - F_\infty^{(2)} = 0 \qquad n \geqslant 3. \tag{12d}$$

Using (8), (9) and (10) we obtain

$$F_0 - F_\infty = -3Ks + 6Ks(1 + 2x^3)\omega^{q_\perp} + 8(1 - x^3)^2\omega^{2q_\perp - 1} - 9(1 - x^3)^2\omega^{2q_\perp} + O(\omega^{3q_- - 4}) \tag{13a}$$

$$F_1 - F_\infty = -6Ks(1 - x^3)\omega^{q_\perp} + (1 - x^3)^2(4 - 5\omega)\omega^{2q_\perp - 1} + O(\omega^{3q_\perp - 3}) \tag{13b}$$

$$F_2 - F_\infty \sim O(\omega^{3q_\perp - 1}). \tag{13c}$$

On the boundary between $n = 0$ and $n = \infty$, defined in first order by (11*a*), $F_1 - F_\infty$ is positive. Hence the $n = 1$ phase must be stable in its vicinity.

The new boundaries which appear to this order between the interface phases with $n = 0$, 1 and ∞ follow immediately from (13*a*) and (13*b*) to be

$$0:1 \qquad 3Ks_{0:1} = (1 - x^3)^2(4 - 4\omega)\omega^{2q_- - 1} + O(\omega^{3q_- - 4}) \tag{14a}$$

$$1:\infty \qquad 3Ks_{1:\infty} = \tfrac{1}{2}(1 - x^3)(4 - 5\omega)\omega^{q_\perp - 1} + O(\omega^{2q_\perp - 3}). \tag{14b}$$

Table 2. Disconnected configurations have been grouped with the corresponding connected configurations. A vertical or horizontal bar denotes a disconnection.

(*a*) Second-order contributions to $F_0 - F_\infty$.

	Configuration	Count	Boltzmann weight
1	$00\ 01$	-4	$(1+xy+2x^{-1}y^2)\omega^{2q_\perp}$
	$00\|01$	4	$(1+x^{-1}y^2)2xy\omega^{2q_\perp}$
2	$00\ 11$	-2	$(3xy+x^{-1}y^2)\omega^{2q_-}$
	$00\|11$	2	$(1+x^{-1}y^2)^2\omega^{2q_-}$
3	$00\ 22$	1	$(3xy+x^2y^{-1})\omega^{2q_-}$
	$00\|22$	-1	$(1+x^2y^{-1})^2\omega^{2q_\perp}$
4	$00\ 02$	2	$(1+2x^2y^{-1}+xy)\omega^{2q_\perp}$
	$00\|02$	-2	$(1+x^2y^{-1})2xy\omega^{2q_\perp}$
5	$00\ 00$	3	$(2xy+x^3+y^3)\omega^{2q_\perp}$
	$00\|00$	-3	$(2xy)^2\omega^{2q_-}$
6	001	-8	$(1+x^{-2}y^4)\omega^{2q_--2}+2x^{-1}y^2\omega^{2q_\perp-1}$
	001		
	$0\underline{0}1$	10	$(1+x^{-1}y^2)^2\omega^{2q_-}$
	001		
7	002	4	$(1+x^4y^{-2})\omega^{2q_\perp-2}+2x^2y^{-1}\omega^{2q_--1}$
	002		
	$0\underline{0}2$	-5	$(1+x^2y^{-1})^2\omega^{2q_\perp}$
	002		
8	000	4	$2x^2y^2(\omega^{2q_\perp-2}+\omega^{2q_--1})$
	000		
	$0\underline{0}0$	-5	$(2xy)^2\omega^{2q_\perp}$
	000		

(*b*) Second-order contributions to $F_1 - F_\infty$.

	Configuration	Count	Boltzmann weight
1	0001	-2	$(1+xy+2x^{-1}y^2)\omega^{2q_-}$
	$00\|01$	2	$(2xy+2y^3)\omega^{2q_\perp}$
2	0011	-2	$(3xy+x^{-1}y^2)\omega^{2q_-}$
	$00\|11$	2	$(1+x^{-2}y^4+2x^{-1}y^2)\omega^{2q_-}$
3	0012	2	$(1+2x^{-1}y^2+x^{-2}y)\omega^{2q_\perp}$
	$00\|12$	-2	$(2x^{-2}y+2x^{-3}y^3)\omega^{2q_\perp}$
4	0000	2	$(2xy+x^3+y^3)\omega^{2q_-}$
	$00\|00$	-2	$4x^2y^2\omega^{2q_-}$
5	001	-4	$(1+x^{-2}y^4)\omega^{2q_--2}+2x^{-1}y^2\omega^{2q_\perp-1}$
	001		
	$0\underline{0}1$	5	$(1+x^{-2}y^4+2x^{-1}y^2)\omega^{2q_\perp}$
	001		
6	012	2	$2x^{-4}y^2(\omega^{2q_\perp-2}+\omega^{2q_--1})$
	012		
	$0\underline{1}2$	$-\frac{5}{2}$	$4x^{-4}y^2\omega^{2q_\perp}$
	012		
7	000	2	$2x^2y^2(\omega^{2q_\perp-2}+\omega^{2q_\perp-1})$
	000		
	$0\underline{0}0$	$-\frac{5}{2}$	$4x^2y^2\omega^{2q_\perp}$
	000		

Table 2. (continued).

(*c*) Second-order contributions to $F_2 - F_\infty$.

	Configuration	Count	Boltzmann weight
1	0001	−2	$(1+xy+2x^{-1}y^2)\omega^{2q_-}$
	00|01	2	$(2xy+2y^3)\omega^{2q_+}$
2	0112	1	$(3x^{-2}y+x^{-1}y^2)\omega^{2q_\perp}$
	01|12	−1	$(1+x^{-2}y^4+2x^{-1}y^2)\omega^{2q_+}$
3	0000	1	$(2xy+x^3+y^3)\omega^{2q_\perp}$
	00|00	−1	$4x^2y^2\omega^{2q_-}$

The boundaries are plotted in figure 1 for $J = J_0$. On the $1:\infty$ boundary all phases with $n \geqslant 1$ remain degenerate and we must consider higher-order terms in the series expansion to test their stability.

2.4. Third order

The third-order contributions to the energy differences $F_1 - F_\infty$, $F_2 - F_\infty$ and $F_3 - F_\infty$ are shown in tables 3(*a*), (*b*) and (*c*). Boltzmann weights depend on three flipped spins, which give a large number of possible graphs. These results have been displayed explicitly because it will be useful in § 3 to distinguish between the various contributions to the free energy difference. From the results in the tables one finds that on the boundary between $n = 1$ and $n = \infty$

$$F_2 - F_\infty = \tfrac{1}{2}(1-x^3)^3(4-5\omega)\omega^{3q_- - 1} + O(\omega^{4q_\perp - 3}) \tag{15a}$$

$$F_3 - F_\infty \sim O(\omega^{4q_\perp - 1}) \qquad n = 3. \tag{15b}$$

The expression in (15*a*) is positive and hence the $n = 2$ phase is stabilised at this order of the expansion.

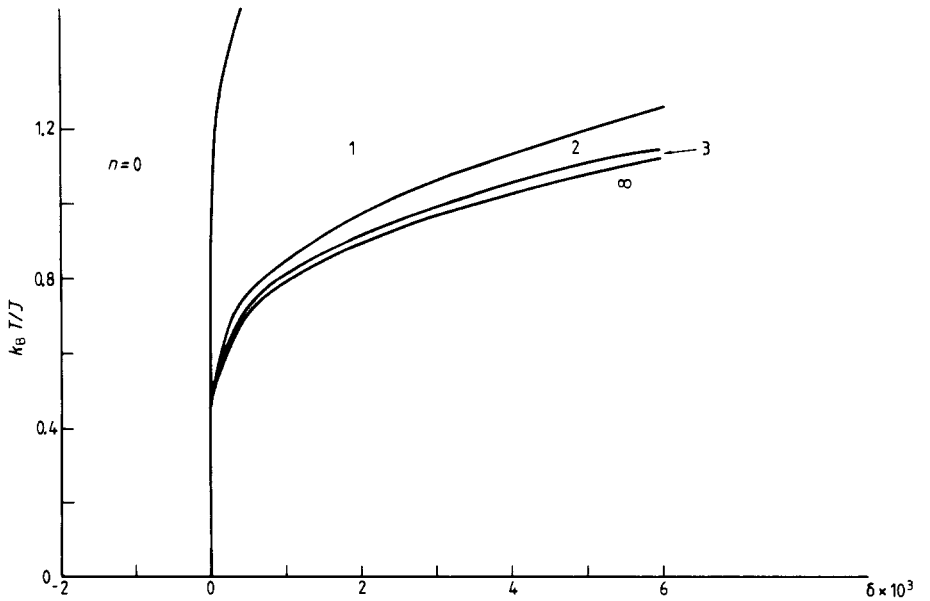

Figure 1. Boundaries between different interface phases calculated for $J_0 = J = 1$ including terms to fourth order.

The boundaries defined to this order between the interface phases with $n=1$, 2 and ∞ follow immediately to be

$$1:2 \qquad 3Ks_{1:2}=\tfrac{1}{2}(1-x^3)(4-5\omega)\omega^{q_\perp-1}+O(\omega^{2q_\perp-3}) \tag{16a}$$

$$2:\infty \qquad 3Ks_{2:\infty}=\tfrac{2}{3}(1-x^3)(4-5\omega)\omega^{q_\perp-1}+O(\omega^{2q_\perp-3}). \tag{16b}$$

On the $2:\infty$ boundary all phases with $n\geqslant 2$ remain degenerate and again we must consider higher-order terms in the series expansion to test their stability. An explicit calculation rapidly becomes impossible, but we now show that it is possible to pick out the important terms at each order of the series expansion.

3. General order

To proceed with the calculation, and build up the interfacial phase diagram, we need to establish the leading-order contribution to F_n-F_∞ (Fisher and Selke 1980, 1981, Yeomans and Fisher 1984). It is intuitively obvious that the important graphs must span the distance between the two interfaces. The lowest-order graphs to do this will be chains of n spins parallel to the axial direction, as shown in figure 2(a). Four such graphs remain when the difference in free energies is taken. These are listed for $n=2$ in table 2(c) and for $n=3$ in table 3(c). It is also apparent from the tables that we must consider all disconnected decompositions of the connected graphs, with each m-fold decomposition contributing a factor $(-1)^m$ (Fisher and Selke 1981).

To count all contributions from such axial graphs of general length together with their decompositions it is possible to use a transfer matrix method introduced by

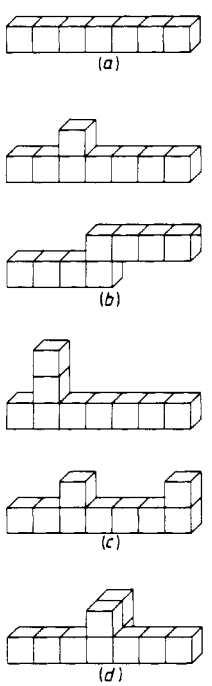

Figure 2. Graphs based on axially connected chains of n spins which contribute to F_n-F_∞ to order (a) $\omega^{nq_\perp}$, (b) $\omega^{(n+1)q_\perp}$, (c) $\omega^{(n+2)q_\perp-4}$ and (d) $\omega^{(n+3)q_\perp-8}$.

Table 3. Disconnected configurations have been grouped with the corresponding connected configurations. A vertical or horizontal bar denotes a disconnection.

(*a*) Third-order contribution to $F_1 - F_\infty$.

	Configuration	Count	Boltzmann weight
1	0*0*0*0*1	−2	$(1+3xy+3x^{-1}y^2+y^3)\omega^{3q_-}$
	0*0*|0*0*1	2	$(1+xy+2x^{-1}y^2)2xy\omega^{3q_-}$
	0*0*0|0*1	2	$(1+x^{-1}y)(2xy+x^3+y^3)\omega^{3q_-}$
	0*0*|0|0*1	−2	$(2xy)^2(1+x^{-1}y^2)\omega^{3q_+}$
2	0*0*0*1*1	−4	$(4xy+x^3+2y^3+x^{-1}y^2)\omega^{3q_-}$
	0*0*0|1*1	4	$(1+xy+2x^{-1}y^2)(1+x^{-1}y^2)\omega^{3q_-}$
	0*0*|0*1*1	4	$(3xy+x^{-1}y^2)2xy\omega^{3q_-}$
	0*0*|0|1*1	−4	$(1+x^{-1}y^2)^2 2xy\omega^{3q_-}$
3	0*0*0*1*2	2	$(2+xy+3x^{-1}y^2+yx^{-2}+x^{-2}y^4)\omega^{3q_-}$
	0*0*0|1*2	−2	$(1+xy+2x^{-1}y^2)2x^{-2}y\omega^{3q_-}$
	0*0*|0*1*2	−2	$(1+2x^{-1}y^2+x^{-2}y)2xy\omega^{3q_-}$
	0*0*|0|1*2	2	$(4x^{-1}y^2)(1+x^{-1}y^2)\omega^{3q_+}$
4	0*0*1*2*2	1	$(4xy+4x^{-1}y^2)\omega^{3q_-}$
	0*0*1|2*2	−1	$(1+x^{-1}y^2)(1+x^{-2}y+2x^{-1}y^2)\omega^{3q_-}$
	0*0*|1*2*2	−1	$(1+x^{-1}y^2)(1+x^{-2}y+2x^{-1}y^2)\omega^{3q_-}$
	0*0*|1|2*2	1	$(1+x^{-1}y^2)^2 2x^{-2}y\omega^{3q_-}$
5	0*0*0*0*0	3	$(2xy+2x^3+2y^3+2x^2y^2)\omega^{3q_-}$
	0*0*0|0*0	−3	$(2xy+x^3+y^3)2xy\omega^{3q_-}$
	0*0*|0*0*0	−3	$(2xy+x^3+y^3)2xy\omega^{3q_-}$
	0*0*|0|0*0	3	$(2xy)^3\omega^{3q_-}$
6	0*0*0*1	−8	$(1+x^{-1}y^2+y^3+x^{-2}y^4)\omega^{3q_-2}+(xy+2x^{-1}y^2+x^{-2}y^4)\omega^{3q_--1}$
	0*0*0*1		
	0*0*0*1	8	$[(1+x^{-2}y^4)\omega^{3q_+-2}+2x^{-1}y^2\omega^{3q_+-1}]2xy$
	0*0*0*1		
	0*0*$\underline{0}$*1	10	$(1+xy+2x^{-1}y^2)(1+x^{-1}y^2)\omega^{3q_-}$
	0*0*|0*1		
	0*0* $\underline{0}$*1	−10	$(1+x^{-1}y^2)^2 2xy\omega^{3q_-}$
	0*0*|0*1		
7	0*0*0*1	−8	$(xy+x^2y^2+2y^3)(\omega^{3q_+-2}+\omega^{3q_+-1})$
	0*0*0*1		
	0*0* 0*1	8	$(1+x^{-1}y^2)2x^2y^2(\omega^{3q_+-2}+\omega^{3q_+-1})$
	0*0*|0*1		
	0$\underline{0}$*0*1	10	$(1+xy+2x^{-1}y^2)2xy\omega^{3q_-}$
	0*0*0*1		
	0$\underline{0}$ *0*1	−10	$(2xy)^2(1+x^{-1}y^2)\omega^{3q_+}$
	0*0*|0*1		
8	0*0*1*1	−16	$(2xy+y^3+x^{-2}y^4)\omega^{3q_--2}+(2y^3+xy+x^{-1}y^2)\omega^{3q_+-1}$
	0*0*1*1		
	0*0* 1*1	16	$(1+x^{-1}y^2)[(1+x^{-2}y^4)\omega^{3q_+-2}+2x^{-1}y^2\omega^{3q_+-1}]$
	0*0*|1*1		
	0$\underline{0}$*1*1	20	$(1+x^{-1}y^2)(3xy+x^{-1}y^2)\omega^{3q_-}$
	0*0*1*1		
	0$\underline{0}$ *1*1	−20	$(1+x^{-1}y^2)^3\omega^{3q_-}$
	0*0*|1*1		
9	0*0*1*2	8	$(x^{-1}y^2+1+x^{-3}y^3+x^{-2}y^4)\omega^{3q_+-2}+(2x^{-1}y^2+x^{-2}y+x^{-2}y^4)\omega^{3q_+-1}$
	0*0*1*2		
	0*0* 1*2	−8	$2x^{-2}y[(1+x^{-2}y^4)\omega^{3q_+-2}+2x^{-1}y^2\omega^{3q_+-1}]$
	0*0*|1*2		
	0$\underline{0}$*1*2	−10	$(1+x^{-1}y^2)(1+x^{-2}y+2x^{-1}y^2)\omega^{3q_+}$
	0*0*1*2		
	0$\underline{0}$ *1*2	10	$(1+x^{-1}y^2)^2 2x^{-2}y\omega^{3q_-}$
	0*0*|1*2		

Table 3. (continued).

	Configuration	Count	Boltzmann weight
10	0012	8	$(x^{-2}y+x^{-4}y^2+2x^{-3}y^3)(\omega^{3q_-\,-2}+\omega^{3q_\perp\,-1})$
	0012		
	001$\underline{2}$	−10	$2x^{-2}y(1+2x^{-1}y^2+x^{-2}y)\omega^{3q_-}$
	0012		
	00 12	−8	$2x^{-4}y^2(1+x^{-1}y^2)(\omega^{3q_\perp\,-2}+\omega^{3q_-\,-1})$
	00|12		
	00 $\underline{1}$2	10	$(1+x^{-1}y^2)(2x^{-2}y)^2\omega^{3q_-}$
	00|12		
11	0000	16	$(2x^2y^2+x^4y+xy^4)(\omega^{3q_-\,-2}+\omega^{3q_-\,-1})$
	0000		
	00$\underline{0}$0	−20	$(2xy+x^3+y^3)2xy\omega^{3q_\perp}$
	0000		
	00 00	−16	$4x^3y^3(\omega^{3q_\perp\,-2}+\omega^{3q_-\,-1})$
	00|00		
	00 $\underline{0}$0	20	$(2xy)^3\omega^{3q_\perp}$
	00|00		
12	001		
	001	−12	$(1+x^{-3}y^6)\omega^{3q_-\,-4}+(x^{-1}y^2+x^{-2}y^4)(2\omega^{3q_\perp\,-3}+\omega^{3q_-\,-2})$
	001		
	001		
	00$\underline{1}$	32	$(1+x^{-1}y^2)[(1+x^{-2}y^4)\omega^{3q_-\,-2}+2x^{-1}y^2\omega^{3q_\perp\,-1}]$
	001		
	00$\underline{1}$		
	00$\underline{1}$	$-\frac{62}{3}$	$(1+x^{-1}y^2)^3\omega^{3q_\perp}$
	001		
13	012		
	012	6	$(x^{-2}y)^3(2\omega^{3q_\perp\,-4}+4\omega^{3q_-\,-3}+2\omega^{3q_\perp\,-2})$
	012		
	012		
	01$\underline{2}$	−16	$4x^{-6}y^3(\omega^{3q_\perp\,-2}+\omega^{3q_\perp\,-1})$
	012		
	01$\underline{2}$		
	01$\underline{2}$	$-\frac{31}{3}$	$(2x^{-2}y)^3\omega^{3q_\perp}$
	012		
14	000		
	000	6	$(2\omega^{3q_\perp\,-4}+4\omega^{3q_\perp\,-3}+2\omega^{3q_\perp\,-2})(xy)^3$
	000		
	000		
	00$\underline{0}$	−16	$4x^3y^3(\omega^{3q_-\,-2}+\omega^{3q_\perp\,-1})$
	000		
	00$\underline{0}$		
	00$\underline{0}$	$\frac{31}{3}$	$(2xy)^3\omega^{3q_\perp}$
	000		

(*b*) Third-order contribution to $F_2 - F_\infty$.

	Configuration	Count	Boltzmann weight
1	00001	−2	$(1+3xy+3x^{-1}y^2+y^3)\omega^{3q_-}$
	00|001	2	$(1+xy+2x^{-1}y^2)2xy\omega^{3q_-}$
	000|01	2	$(1+x^{-1}y)(2xy+x^3+y^3)\omega^{3q_\perp}$
	00|0|01	−2	$(2xy)^2(1+x^{-1}y^2)\omega^{3q_-}$
2	00011	−2	$(4xy+x^3+2y^3+x^{-1}y^2)\omega^{3q_-}$
	00|011	2	$(3xy+x^{-1}y^2)2xy\omega^{3q_\perp}$
	000|11	2	$(1+xy+2x^{-1}y^2)(1+x^{-1}y^2)\omega^{3q_-}$
	00|0|11	−2	$(1+x^{-1}y^2)^2 2xy\omega^{3q_\perp}$

Table 3. (continued).

	Configuration	Count	Boltzmann weight
3	00112	2	$(1+xy+5x^{-1}y^2+yx^{-2})\omega^{3q_-}$
	00|112	−2	$(3x^{-2}y+x^{-1}y^2)(1+x^{-1}y^2)\omega^{3q_+}$
	001|12	−2	$(3xy+x^{-1}y^2)(1+x^{-1}y^2)\omega^{3q_-}$
	00|1|12	2	$(1+x^{-1}y^2)^3\omega^{3q_+}$
4	00000	2	$(2xy+2x^3+2y^3+2x^2y^2)\omega^{3q_-}$
	00|000	−2	$(2xy+x^3+y^3)2xy\omega^{3q_-}$
	0000|0	−2	$(2xy+x^3+y^3)2xy\omega^{3q_-}$
	00|0|00	2	$(2xy)^3\omega^{3q_-}$
5	0001	−8	$(xy+x^2y^2+2y^3)(\omega^{3q_+-2}+\omega^{3q_--1})$
	0001		
	0001	8	$(1+x^{-1}y^2)2x^2y^2(\omega^{3q_+-2}+\omega^{3q_--1})$
	00|01		
	0001	10	$(1+xy+2x^{-1}y^2)2xy\omega^{3q_+}$
	0001		
	0001	−10	$(2xy)^2(1+x^{-1}y^2)\omega^{3q_-}$
	00|01		
6	0001	−8	$(1+x^{-1}y^2+y^3+x^{-2}y^4)\omega^{3q_+-2}+(xy+2x^{-1}y^2+x^{-2}y^4)\omega^{3q_--1}$
	0001		
	00 01	8	$[(1+x^{-2}y^4)\omega^{3q_+-2}+2x^{-1}y^2\omega^{3q_--1}]2xy$
	00|01		
	0001	10	$(1+xy+2x^{-1}y^2)(1+x^{-1}y^2)\omega^{3q_-}$
	0001		
	0001	−10	$(1+x^{-1}y^2)^2 2xy\omega^{3q_-}$
	00|01		
7	0112	8	$(x^{-3}y^3+x^{-2}y^4+2x^{-2}y)\omega^{3q_+-2}+(x^{-2}y+x^{-1}y^2+2x^{-3}y^3)\omega^{3q_--1}$
	0112		
	01 12	−8	$(1+x^{-1}y^2)((1+x^{-2}y^4)\omega^{3q_+-2}+2x^{-1}y^2\omega^{3q_+-1})$
	01|12		
	0112	−10	$(3x^{-2}y+x^{-1}y^2)(1+x^{-1}y^2)\omega^{3q_+}$
	0112		
	01 12	10	$(1+x^{-1}y^2)^3\omega^{3q_+}$
	01|12		
8	0000	8	$(2x^2y^2+x^4y+xy^4)(\omega^{3q_+-2}+\omega^{3q_--1})$
	0000		
	00 00	−8	$4x^3y^3(\omega^{3q_+-2}+\omega^{3q_--1})$
	00|00		
	0000	−10	$(2xy+x^3+y^3)2xy\omega^{3q_+}$
	0000		
	00 00	10	$(2xy)^3\omega^{3q_+}$
	00|00		

(*c*) Third-order contributions to $F_3 - F_\infty$.

	Configuration	Count	Boltzmann weight
1	00001	−2	$(1+3xy+3x^{-1}y^2+y^3)\omega^{3q_-}$
	00|001	2	$(1+xy+2x^{-1}y^2)2xy\omega^{3q_+}$
	000|01	2	$(1+x^{-1}y)(2xy+x^3+y^3)\omega^{3q_+}$
	00|0|01	−2	$(2xy)^2(1+x^{-1}y^2)\omega^{3q_+}$
2	01112	1	$(4x^{-2}y+4x^{-1}y^2)\omega^{3q_+}$
	011|12	−1	$(1+x^{-1}y^2)(1+xy+2x^{-1}y^2)\omega^{3q_-}$
	01|112	−1	$(1+x^{-1}y^2)(1+xy+2x^{-1}y^2)\omega^{3q_+}$
	01|1|12	1	$2xy(1+x^{-1}y^2)^2\omega^{3q_+}$
3	00000	1	$(2xy+2x^3+2y^3+2x^2y^2)\omega^{3q_+}$
	000|00	−1	$(2xy+x^3+y^3)2xy\omega^{3q_+}$
	00|000	−1	$(2xy+x^3+y^3)2xy\omega^{3q_+}$
	00|0|00	1	$(2xy)^3\omega^{3q_-}$

Yeomans and Fisher (1984). This allows the chain of flipped spins to be built up step by step with the appropriate Boltzmann factor for a connected or disconnected spin being included at each stage. Details of the method are given in appendix 1 of this paper.

Using (9) and (10) in the matrix products, we find that there is, in fact, a zero contribution to order n, but to order $n+1$,

$$(F_n^{(n)} - F_\infty^{(n)})' = -(1+n)3Ks(1-x^3)^n\omega^{nq_\perp} \tag{17}$$

where $'$ indicates that we are only considering a subset of the contributions to the free energy difference because new graphs will also be important to order $n+1$. These are axially connected chains of length n with a single protruding spin on the side, as shown in figure 2(b). These graphs, together with their decompositions, are shown for $F_2 - F_\infty$ at third order in table 3(b). The leading-order contributions from them may be calculated using an extended version of the transfer matrix which is described in appendix 2. One obtains, putting $y = x^2$,

$$(F_n^{(n+1)} - F_\infty^{(n+1)})' = n(1-x^3)^{n+1}(4-5\omega)\omega^{(n+1)q_\perp - 1}. \tag{18}$$

Summing (17) and (18) gives

$$F_n - F_\infty = -3Ks(1+n)(1-x^3)^n\omega^{nq_\perp} + n(1-x^3)^{n+1}(4-5\omega)\omega^{(n+1)q_\perp - 1} + O(\omega^{(n+2)q_\perp - 3}). \tag{19}$$

The correction term in (19) (and indeed in (14), (15) and (16)) deserves some comment as one would naively expect it to be $\omega^{(n+2)q_\perp - 4}$ and $\omega^{(n+3)q_\perp - 8}$ due to corrections from graphs such as those shown in figure 2(c) and 2(d) where the protruding spins flip to the same state as their neighbours. It is, however, shown in appendix 3 that these give zero contribution.

We now build up the phase diagram to general order by an inductive argument. Consider the point at which the phase $(n-1)$ has just become stable. From (19) one finds the phase boundary between $(n-1)$ and ∞ to be

$$3Ks_{n-1:\infty} = (1-x^3)\left(\frac{n-1}{n}\right)(4-5\omega)\omega^{q_\perp - 1} + O(\omega^{2q_\perp - 3}). \tag{20}$$

The nth phase is stable if $F_n - F_\infty$ is positive along the $n-1:\infty$ boundary. Putting $s = s_{n-1:\infty}$, $F_n - F_\infty$ is given by

$$F_n - F_\infty = \frac{(1-x^3)^{n+1}}{n}\omega^{(n+1)q_\perp - 1} + O(\omega^{(n+2)q_\perp - 3}). \tag{21}$$

This is positive, so therefore the nth phase is stable, and we go on to build up a sequence of layering transitions. The width of the nth phase is given by

$$3Ks_{n:n+1} - 3Ks_{n-1:n} = \frac{(1-x^3)}{n(n+1)}(4-5\omega)\omega^{q_\perp - 1} + O(\omega^{2q_\perp - 3}) \tag{22}$$

which is a rapidly decreasing function of n. Note that it would not be valid to deduce that there are an infinite number of layering transitions, as the correction terms may become important when $n^{-1} \sim O(\omega)$ and the sequence may terminate at some finite n.

4. Conclusion

We have shown that a low temperature series for the three-dimensional three-state chiral clock model predicts wetting proceeds via a series of layering transitions. A

similar phenomenon was first predicted by de Oliveira and Griffiths (1978) who used mean-field theory to show that an interface unbinds from a surface through a series of first-order transitions as the bulk field tends to zero. More recently Duxbury and Yeomans (1985) demonstrated that these results could be reproduced using low temperature series and that, for the Abraham (1980) model, where the interface is bound by a row of weak bonds at the surface, at least two layering transitions occur.

At higher temperatures we expect the wetting transition to be continuous as, above the roughening temperature, it is not possible to distinguish between different layers. This is indeed the situation found by Huse *et al* (1983) for the two-dimensional chiral clock model. We also note that, although the two-dimensional wetting line of Huse *et al* (1983) curves to smaller Δ as the temperature is increased, the three-dimensional results indicate a curve to larger Δ. This is because of the role of roughening in two dimensions: the interfaces try to perform infinite fluctuations about their mean positions and hence repel each other. In three dimensions, at low temperatures, however, the interfaces are not rough and fluctuations are not so large. The lowest-order contribution to the free energy (and indeed the mechanism for the multilayer adsorption) is from correlated fluctuations. Hence there is an effective attraction of the interfaces near $\Delta = \frac{1}{4}$.

We are at present studying wetting in the chiral clock model using a mean-field theory. The mean-field results, which will be presented elsewhere, show a first-order transition to $n = 1$, followed by a transition to $n = \infty$.

Acknowledgments

The support of the SERC, in the form of a Research Studentship, is gratefully acknowledged by KA. We also thank M E Fisher for useful and interesting conversations.

Appendices. The matrix method

In these appendices we explain how to calculate the diagrams which contribute to the interface free energy to leading order. We first consider axially connected chains and then chains with a single kink or bump as shown in figures 2(a) and 2(b) respectively. We then show that configurations corresponding to a double kink or bump (figure 2(c)) give zero contribution $O(\omega^{(n+2)q_\perp - 4})$.

Appendix 1. Axial chains of length n

A1.1. Middle matrices

The transfer matrix method for calculating the Boltzmann factor associated with chains of length n has been described in Yeomans and Fisher (1984). We therefore limit ourselves to a brief outline of the method and a list of the transfer matrices appropriate to the problem in hand. The idea is to use a transfer matrix to record the Boltzmann factors as a line of flipped spins is sequentially built up. Consider, for example, adding the bond between two spins, a and b, in state 0. Each spin may flip to two possible

states, 1 and 2, and the corresponding Boltzmann factors may be recorded in matrix form:

$$\mathbf{M}' = \text{spin } a \begin{matrix} \\ 1 \\ 2 \end{matrix} \begin{matrix} \text{spin } b \\ \begin{matrix} 1 & 2 \end{matrix} \end{matrix} \begin{bmatrix} 1 & x \\ y & 1 \end{bmatrix} \omega^{q_\perp}. \tag{A1.1}$$

There is also the possibility of spins a and b being disconnected. This involves a negative contribution to the weights (Yeomans and Fisher 1984)

$$\mathbf{M}'' = \text{spin } a \begin{matrix} \\ 1 \\ 2 \end{matrix} \begin{matrix} \text{spin } b \\ \begin{matrix} 1 & 2 \end{matrix} \end{matrix} \begin{bmatrix} -xy & -y^2 \\ -x^2 & -xy \end{bmatrix} \omega^{q_\perp} \tag{A1.2}$$

where, for example, xy which appears in the top left-hand corner of the matrix is the product of the Boltzmann factors associated with $0\text{-}0 \rightarrow 0\text{-}1$ and $0\text{-}0 \rightarrow 1\text{-}0$.

Hence the total contribution of a 0-0 bond is

$$\mathbf{M} = \mathbf{M}' + \mathbf{M}'' = \begin{matrix} \\ 1 \\ 2 \end{matrix} \begin{matrix} \begin{matrix} 1 & 2 \end{matrix} \\ \begin{bmatrix} 1-xy & x-y^2 \\ y-x^2 & 1-xy \end{bmatrix} \end{matrix} \omega^{q_\perp}. \tag{A1.3}$$

We shall also need the matrix that adds a 0-1 bond:

$$\mathbf{N} = \begin{matrix} \\ 1 \\ 2 \end{matrix} \begin{matrix} \begin{matrix} 2 & 0 \end{matrix} \\ \begin{bmatrix} 1-x^{-2}y & x^{-1}y-x^{-2} \\ x^{-1}-x^{-2}y^2 & 1-x^{-2}y \end{bmatrix} \end{matrix} \omega^{q_\perp}. \tag{A1.4}$$

A1.2. Initial vectors

The initial bond in a chain is added by a row vector. The configurations we shall require are

$$\underline{0\text{-}0} \qquad \boldsymbol{M}_i = \begin{matrix} 0 \\ \\ \end{matrix} \begin{matrix} \begin{matrix} 1 & 2 \end{matrix} \\ \begin{bmatrix} x & y \end{bmatrix} \end{matrix} \omega^{q_\perp} \tag{A1.5}$$

$$\underline{0\text{-}1} \qquad \boldsymbol{N}_i = \begin{matrix} 0 \\ \\ \end{matrix} \begin{matrix} \begin{matrix} 2 & 0 \end{matrix} \\ \begin{bmatrix} x^{-1}y & x^{-1} \end{bmatrix} \end{matrix} \omega^{q_\perp}. \tag{A1.6}$$

A1.3. Final vectors

Similarly the final spin is added by a column vector. (A factor $\omega^{q_\perp}$ is not now necessary as no in-layer bond is added.)

$$\underline{0\text{-}0} \qquad \begin{matrix} \\ 0 \\ \\ \end{matrix} \begin{bmatrix} y \\ x \end{bmatrix} \qquad \underline{0\text{-}1} \qquad \begin{matrix} \\ 1 \\ \\ \end{matrix} \begin{bmatrix} x^{-1} \\ x^{-1}y \end{bmatrix}. \tag{A1.7}$$

A1.4. Matrix products

We expect the leading contributions to the difference in free energies to be associated with axial chains of length n which connect the two interfaces. The total Boltzmann

factor for such chains of spins may now be calculated by forming products of the matrices listed above. As explained in the text the spin chains which contribute to $F_n - F_\infty$ in nth order, together with their corresponding matrix products, are

Configuration (the italics contain n spins)	Count	Matrix product
$0111\ldots1112$	1	$\boldsymbol{N}_i\mathbf{M}^{n-1}\boldsymbol{N}_f$
$0000\ldots0001$	−1	$\boldsymbol{M}_i\mathbf{M}^{n-1}\boldsymbol{N}_f$
$0111\ldots1111$	−1	$\boldsymbol{N}_i\mathbf{M}^{n-1}\boldsymbol{M}_f$
$0000\ldots0000$	1	$\boldsymbol{M}_i\mathbf{M}^{n-1}\boldsymbol{M}_f$.

(A1.8)

Hence

$$F'_n - F'_\infty = (\boldsymbol{N}_i - \boldsymbol{M}_i)(\mathbf{M}^{n-1})(\boldsymbol{N}_f - \boldsymbol{M}_f). \tag{A1.9}$$

Performing the products, summing over the appropriate counts and using (9) and (10) gives

$$F'_n - F'_\infty = \alpha \log x(1+n)(1-x^3)^n\omega^{nq_-} + O(\omega^{(n+2)q_\perp - 2}). \tag{A1.10}$$

Hence the $O(\omega^{nq_-})$ contribution to $F_n - F_\infty$ is zero, and the leading-order term in the free energy difference will be $\sim\alpha(\log x)\omega^{nq_\perp} \sim \omega^{(n+1)q_\perp - 1}$. The prime on the free energies is used to indicate that we must include other contributions at this order.

A1.5. Axial chains of length $n+1$

Because the leading-order term in the free energy difference is $O(\omega^{(n+1)q_\perp - 1})$ we must also consider contributions from axial chains of length $n+1$. Those which contribute to the free energy difference (see, for example, table 3(b)) are

Configuration (the italics contain $n+1$ spins)	Count	Matrix product
$0000\ldots0001$	−2	$\boldsymbol{M}_i\mathbf{M}^{n}\boldsymbol{N}_f$
$0000\ldots0011$	−2	$\boldsymbol{M}_i\mathbf{M}^{n-1}\mathbf{N}\boldsymbol{M}_f$
$0111\ldots1122$	2	$\boldsymbol{N}_i\mathbf{M}^{n-1}\mathbf{N}\boldsymbol{M}_f$
$0000\ldots0000$	2	$\boldsymbol{M}_i\mathbf{M}^{n}\boldsymbol{M}_f$.

(A1.11)

Summing the matrix products and specialising to $y = x^2$ to obtain the leading order gives

$$F'_n - F'_\infty = 0 + O(\omega^{(n+2)q_- - 1}). \tag{A1.12}$$

Therefore axial chains of length $(n+1)$ do not contribute in leading order. However, we must consider other contributions.

Appendix 2. Axial chains with a single kink or bump

We now show how to calculate the configurations shown in figure 2(b) which also contribute to $F_n - F_\infty$ at order $n+1$. The easiest way to deal with these seems to be to consider sparse 8×8 matrices which add the Boltzmann factors of the bonds between two adjacent spins in each of two consecutive layers, together with the in-layer bonds in the right-hand layer. Note that the matrices will only give the correct *leading-order* term when multiplied together.

A2.1. Middle matrices

We consider, as an example, the matrix which connects two zero layers

$$
\begin{array}{c}
0\text{—}0 \\
| \\
0\text{—}0
\end{array}
$$

$$
\begin{array}{c|cccccccccc}
 & \begin{matrix}1\\0\end{matrix} & \begin{matrix}2\\0\end{matrix} & \begin{matrix}0\\1\end{matrix} & \begin{matrix}0\\2\end{matrix} & 1 & 2 & 1 & 2 & \multicolumn{2}{c}{\multirow{2}{*}{$\omega^{q_\perp}$.}} \\
 & & & & & & & & & & \\
\hline
\begin{matrix}1\\0\end{matrix} & (1-xy) & (x-y^2) & 0 & 0 & 0 & 0 & 0 & 0 & 0 & \\
\begin{matrix}2\\0\end{matrix} & (y-x^2) & (1-xy) & 0 & 0 & 0 & 0 & 0 & 0 & 0 & \\
\begin{matrix}0\\1\end{matrix} & 0 & 0 & (1-xy) & (x-y^2) & \begin{matrix}(x-x^2y)\times\\(4\omega^{q_\perp-2}-5\omega^{q_\perp})\end{matrix} & \begin{matrix}(y-xy^2)\times\\(4\omega^{q_\perp-1}-5\omega^{q_\perp})\end{matrix} & \begin{matrix}(x^2-xy^2)\times\\(4\omega^{q_\perp-1}-5\omega^{q_\perp})\end{matrix} & \begin{matrix}(xy-y^3)\times\\(4\omega^{q_\perp-2}-5\omega^{q_\perp})\end{matrix} & & \\
\begin{matrix}0\\2\end{matrix} & 0 & 0 & (y-x^2) & (1-xy) & \begin{matrix}(yx-x^3)\times\\(4\omega^{q_\perp-2}-5\omega^{q_\perp})\end{matrix} & \begin{matrix}(y^2-x^2y)\times\\(4\omega^{q_\perp-1}-5\omega^{q_\perp})\end{matrix} & \begin{matrix}(x-x^2y)\times\\(4\omega^{q_\perp-1}-5\omega^{q_\perp})\end{matrix} & \begin{matrix}(y-xy^2)\times\\(4\omega^{q_\perp-2}-5\omega^{q_\perp})\end{matrix} & & \\
\begin{matrix}1\\1\end{matrix} & (y-xy^2) & (xy-y^3) & (y-xy^2) & (xy-y^3) & 0 & 0 & 0 & 0 & & \\
\begin{matrix}2\\1\end{matrix} & (y^2-x^2y) & (y-xy^2) & (x-x^2y) & (x^2-xy^2) & 0 & 0 & 0 & 0 & & \\
\begin{matrix}1\\2\end{matrix} & (x-x^2y) & (x^2-xy^2) & (y^2-x^2y) & (y-xy^2) & 0 & 0 & 0 & 0 & & \\
\begin{matrix}2\\2\end{matrix} & (xy-x^3) & (x-x^2y) & (xy-x^3) & (x-x^2y) & 0 & 0 & 0 & 0 & &
\end{array}
\qquad \text{(A2.1)}
$$

To construct the matrix note the following.

(i) The labelling of the rows and columns follows because each spin can flip to state 1 or 2 or remain in its original state. At least one of the two spins must flip, however; hence we need not consider $\begin{smallmatrix}0\\0\end{smallmatrix}$.

(ii) Our aim is to build up the configurations shown in figure 2(b) and variants where the kink or bump moves along the chain or the diagram is rotated about the axial direction. (The linear configurations, considered separately in appendix 1, are also included in this formalism.) We always take the first spin to lie on the lowest line of the pair considered (in terms of how the matrix is labelled) to avoid overcounting. It is then immediately apparent that

(a) the configurations in the bottom right-hand corner of the matrix are not allowed as they contribute in higher order;

(b) zero configurations in the top left-hand corner are disallowed because they correspond to disconnected spin chains, and

(c) the top two rows on the right-hand side of the matrix must correspond to zero entries as configurations such as $\begin{smallmatrix}1&1\\0&1\end{smallmatrix}$ would introduce a second kink into the chain and hence be of higher order.

(iii) We now consider the non-zero portions of the matrix.

(a) The two 2×2 filled blocks in the top left-hand quadrant of the matrix correspond to adding a single axially connected or disconnected spin. They are therefore the same as (A1.3) in appendix 1.

(b) The bottom left-hand quadrant also corresponds to adding a single connected or disconnected spin. Hence the Boltzmann factor of the bond to the flipped spin neighbouring an unflipped spin must also be considered.

(c) The non-zero terms on the right-hand side of the matrix are of a more complicated form because two spins are added and three disconnected configurations must be taken into account. Consider the $\begin{smallmatrix}0&1\\1&1\end{smallmatrix}$ term. This, when connected, corresponds to a factor $4x\omega^{2q_\perp-2}$, the x from the 0-1 bond on the top row (and the 1-1 bond on the bottom row which gives a factor 1), and the $\omega^{2q_\perp-2}$ from the in-layer contribution. The factor of four appears to count the possible rotations of this configuration around the axial direction. If there is a disconnection between the two spins on the bottom row one obtains $-4x^2y\omega^{2q_\perp-2}$. Taking the disconnection to lie between the two bonds in the same layer gives $-5x\omega^{2q_\perp}$. Note the factor five, not four; this occurs because there are five forbidden positions for the disconnected spin. Finally, if both disconnections are present one must add a term $5x^2y\omega^{2q_\perp}$.

The other 8×8 matrix (see opposite page) which we shall need adds two spins in state 1 to two in state 0. This, by similar reasoning, is given by

$$
\begin{array}{c}
\begin{matrix} & & & 0\text{---}1 & & & & \\ & & & | & & & & \\ & & & \underline{0\text{—}1} & & & & \end{matrix} \\
\begin{matrix} 2 & 0 & 1 & 1 & 2 & 0 & 2 & 0 \\ 1 & 1 & 2 & 0 & 2 & 2 & 0 & 0 \end{matrix} \\
\begin{matrix} 1\\0 \\ 2\\0 \\ 0\\1 \\ 0\\2 \\ 1\\1 \\ 2\\1 \\ 1\\2 \\ 2\\2 \end{matrix}
\begin{bmatrix}
(1-x^{-2}y) & (x^{-1}y-x^{-2}) & 0 & 0 & 0 & 0 & 0 & 0 \\
(x^{-1}-x^{-2}y^2) & (1-x^{-2}y) & 0 & 0 & 0 & 0 & 0 & 0 \\
0 & 0 & (1-x^{-2}y) & (x^{-1}y-x^{-2}) & \begin{matrix}(x^{-1}y-x^{-3}y^2)\times\\(4\omega^{q_\perp-2}-5\omega^{q_\perp})\end{matrix} & \begin{matrix}(x^{-1}-x^{-3}y)\times\\(4\omega^{q_\perp-1}-5\omega^{q_\perp})\end{matrix} & \begin{matrix}(x^{-2}y^2-x^{-3}y)\times\\(4\omega^{q_\perp-1}-5\omega^{q_\perp})\end{matrix} & \begin{matrix}(x^{-2}y-x^{-3})\times\\(4\omega^{q_\perp-2}-5\omega^{q_\perp})\end{matrix} \\
0 & 0 & (x^{-1}-x^{-2}y^2) & (1-x^{-2}y) & \begin{matrix}(x^{-2}y-x^{-3}y^3)\times\\(4\omega^{q_\perp-2}-5\omega^{q_\perp})\end{matrix} & \begin{matrix}(x^{-2}-x^{-3}y^2)\times\\(4\omega^{q_\perp-1}-5\omega^{q_\perp})\end{matrix} & \begin{matrix}(x^{-1}y-x^{-3}y^2)\times\\(4\omega^{q_\perp-1}-5\omega^{q_\perp})\end{matrix} & \begin{matrix}(x^{-1}-x^{-3}y)\times\\(4\omega^{q_\perp-2}-5\omega^{q_\perp})\end{matrix} \\
(x^{-1}-x^{-3}y) & (x^{-2}y-x^{-3}) & (x^{-1}-x^{-3}y) & (x^{-2}y-x^{-3}) & 0 & 0 & 0 & 0 \\
(x^{-2}-x^{-3}y^2) & (x^{-1}-x^{-3}y) & (x^{-1}y-x^{-3}y^2) & (x^{-2}y^2-x^{-3}y) & 0 & 0 & 0 & 0 \\
(x^{-1}y-x^{-3}y^2) & (x^{-2}y^2-x^{-3}y) & (x^{-2}-x^{-3}y^2) & (x^{-1}-x^{-3}y) & 0 & 0 & 0 & 0 \\
(x^{-2}y-x^{-3}y^3) & (x^{-1}y-x^{-3}y^2) & (x^{-2}y-x^{-3}y^3) & (x^{-1}y-x^{-3}y^2) & 0 & 0 & 0 & 0
\end{bmatrix}^{\omega^{q_\perp}}
\end{array}
\qquad \text{(A2.2)}
$$

A2.2. Initial vectors

The initial two spins in a given chain are added by the row vectors

$$\begin{array}{c} \\ \\ 0\!-\!0 \\ | \\ \underline{0\!-\!0} \end{array}$$

$$\begin{array}{cccccccccc} & 1 & 2 & 0 & 0 & & 1 & 2 & 1 & 2 \\ & 0 & 0 & 1 & 2 & & 1 & 1 & 2 & 2 \\ 0[& 0 & 0 & x & y & \tfrac{1}{2}x^2(4\omega^{q_--2}-5\omega^{q_-}) & \tfrac{1}{2}xy(4\omega^{q_--1}-5\omega^{q_\perp}) & \tfrac{1}{2}xy(4\omega^{q_--1}-5\omega^{q_-}) & \tfrac{1}{2}y^2(4\omega^{q_\perp-2} & \\ & & & & & & & & -5\omega^{q_\perp})]\omega^{q_\perp} & \end{array} \tag{A2.3}$$

$$\begin{array}{c} \\ \\ 0\!-\!1 \\ | \\ \underline{0\!-\!1} \end{array}$$

$$\begin{array}{cccccccccc} & 2 & 0 & 1 & 1 & & 2 & 0 & 2 & 0 \\ & 1 & 1 & 2 & 0 & & 2 & 2 & 0 & 0 \\ 0[& 0 & 0 & x^{-1}y & x^{-1} & \tfrac{1}{2}x^{-2}y^2(4\omega^{q_--2}-5\omega^{q_-}) & \tfrac{1}{2}x^{-2}y(4\omega^{q_--1}-5\omega^{q_-}) & \tfrac{1}{2}x^{-2}y(4\omega^{q_--1}-5\omega^{q_-}) & \tfrac{1}{2}x^{-2}(4\omega^{q_--2}-5\omega^{q_\perp})]\omega^{q_\perp} & \end{array} \tag{A2.4}$$

The first two entries are zero because we fix the first flipped spin to be the bottom spin and the second two should be compared to (A1.5) and (A1.6). The other terms allow for both spins in the first layer to be flipped and for the possibility of their being disconnected. The factor of two appears because the matrix product counts the diagrams 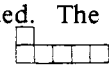 and 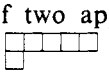 as distinct when this is not the case.

A2.3. Final vectors

The column vectors which add the bonds to the right of the final flipped spins are

$$\begin{array}{c} 0\!-\!0 \\ | \\ \underline{0\!-\!0} \end{array} \qquad \begin{array}{c} 0\!-\!1 \\ | \\ \underline{0\!-\!1} \end{array}$$

$$\begin{array}{cc} & 0 \\ \begin{matrix}1\\0\end{matrix} & y \\ \begin{matrix}2\\0\end{matrix} & x \\ \begin{matrix}0\\1\end{matrix} & y \\ \begin{matrix}0\\2\end{matrix} & x \\ \begin{matrix}1\\1\end{matrix} & y^2 \\ \begin{matrix}2\\1\end{matrix} & xy \\ \begin{matrix}1\\2\end{matrix} & xy \\ \begin{matrix}2\\2\end{matrix} & x^2 \end{array} \qquad \begin{array}{cc} & 1 \\ \begin{matrix}1\\0\end{matrix} & x^{-1} \\ \begin{matrix}2\\0\end{matrix} & x^{-1}y \\ \begin{matrix}0\\1\end{matrix} & x^{-1} \\ \begin{matrix}0\\2\end{matrix} & x^{-1}y \\ \begin{matrix}1\\1\end{matrix} & x^{-2} \\ \begin{matrix}2\\1\end{matrix} & x^{-2}y \\ \begin{matrix}1\\2\end{matrix} & x^{-2}y \\ \begin{matrix}2\\2\end{matrix} & x^{-2}y^2 \end{array} \tag{A2.5}$$

A2.4. Matrix products

To calculate the $(n+1)$th order contribution to $F_n - F_\infty$ we should now use the full matrices which allow for single kinks and bumps on axial chains of length n. The configurations we need consider are exactly those shown in (A1.8) and indeed the results (A1.10) and (A1.12) also follow from using the 8×8 matrices. It is, however, easier to treat the linear chains separately using the smaller matrices as the full dependence on x and y is important, and to put $y = x^2$ in the general case so that only the 'kink and bump' terms survive. If this is done the matrix products simplify considerably and can be performed explicitly to give

$$F'_n - F'_\infty = -3Ks(1+n) \times (1-x^3)^n \omega^{nq_\perp} + n(1-x^3)^{n+1}(4-5\omega)\omega^{(n+1)q_\perp - 1} + O(\omega^{(n+1)q_\perp - 3}). \quad \text{(A2.6)}$$

Appendix 3. Axial chains with two kinks or bumps

As we are considering a cubic lattice we must also count graphs with $(n+2)$ spin flips which can contribute in order $\omega^{(n+2)q_\perp - 4} \sim \omega^{(n+1)q_\perp}$. Such terms are generated by connected or disconnected axial chains of length n, with two kinks or bumps as shown in figure 2(c), if all the overturned spins within a given layer flip to the same state. In-layer disconnections need not be considered. Moreover, $\omega^{(n+3)q_\perp - 8}$ terms, which are also of this order, appear from graphs like that depicted in figure 2(d) if the square of spins all flip to the same state.

In this appendix we show the contribution from these graphs is zero to leading order. This occurs for the same reason as the vanishing of the contribution from axial chains of length n and $n+1$ (see (A1.10) and (A1.12)) to order n and $n+1$ respectively. We first demonstrate why this happens, showing that in fact the matrix product is zero, not only when all possible spin flips are taken into account, but also term by term for each flipped configuration:

$$(n_1 \to n_1 + \alpha_1,\ n_2 \to n_2 + \alpha_2, \ldots n_n \to n_n + \alpha_n) \qquad \alpha_i = \pm 1 \qquad i = 1, 2, \ldots, n$$

when the sum over the four contributing graphs (A1.8) or (A1.11) is taken. Writing out (A1.9) explicitly for $y = x^2$:

$$F'_n - F'_\infty = [0,\ x^{-1} - x](1-x^3)^{n-1} \begin{bmatrix} 1 & x \\ 0 & 1 \end{bmatrix}^n \begin{bmatrix} x^{-1} - x^2 \\ 0 \end{bmatrix} \omega^{nq_-}. \quad \text{(A3.1)}$$

It is immediately apparent that if $\alpha_1 = 1$, $F'_n - F'_\infty = 0$ because the first term in the initial row matrix is zero. If $\alpha_1 = 2$ and $\alpha_2 = 1$, the difference is zero because the matrix has a zero term in the bottom left-hand corner. Similarly if $\alpha_1 = 2$, $\alpha_2 = 2$, $\alpha_3 = 1$, and so on, until for $\alpha_i = 2$ for all i the product must be zero because the bottom term in the column vector is zero. Note that this argument hinges on the zero in the middle matrix which only occurs because both connected and disconnected configurations give the same Boltzmann factors.

We now turn to the case of axial chains with several kinks or bumps. The contribution from any particular diagram may still be written as a product of 2×2 matrices, if M_0 is replaced by a new matrix whenever there is a kink or bump to allow for the additional spins in the layers. For example, the matrix which adds a layer

which includes a kink in the same state is

$$\begin{array}{c} 0 \\ | \\ \underline{0—0} \end{array} \quad \begin{array}{c} \\ 1 \\ 2 \end{array} \begin{array}{c} \begin{array}{cc} 1 & 2 \end{array} \\ \begin{bmatrix} (4x-4x^2y)\omega^{2q_\perp-2} & (4xy-4y^3)\omega^{2q_\perp-2} \\ (4xy-4x^3)\omega^{2q_\perp-2} & (4y-4xy)\omega^{2q_\perp-2} \end{bmatrix}. \end{array} \tag{A3.2}$$

If zeros occur in the new matrices in the same position as in the M_0 the contribution from the matrix product will vanish in the same way as above. By considering the possible allowed diagrams in turn we have found that this is indeed the case for all the graphs O $(\omega^{(n+2)q_\perp-4})$ and O $(\omega^{(n+3)q_\perp-8})$ (though not for $\omega^{(n+2)q_\perp-3}$, etc).

References

Abraham D B 1980 *Phys. Rev. Lett.* **44** 1165
de Gennes P G 1985 *Rev. Mod. Phys.* **57**
de Oliveira M J and Griffiths R B 1978 *Surf. Sci.* **71** 687
Domb C 1960 *Adv. Phys.* **9** 149
Duxbury P M and Yeomans J M 1985 *J. Phys. A: Math. Gen.* **18** L983
Fisher M E and Selke W 1980 *Phys. Rev. Lett.* **44** 1502
—— 1981 *Phil. Trans. R. Soc.* **302** 1
Huse D A 1981 *Phys. Rev.* B **24** 5180
Huse D A and Fisher M E 1984 *Phys. Rev.* B **29** 239
Huse D A, Szpilka A M and Fisher M E 1983 *Physica* **121A** 363
Lipowsky R 1985 *Phys. Rev.* B **32** 1731
Ostlund S 1981 *Phys. Rev.* B **24** 298
Telo da Gama M M 1985 *Fluid Interfacial Phenomena* ed C A Croxton (New York: Wiley)
Yeomans J M and Fisher M E 1984 *Physica* **127A** 1